ChemComm

Accepted Manuscript

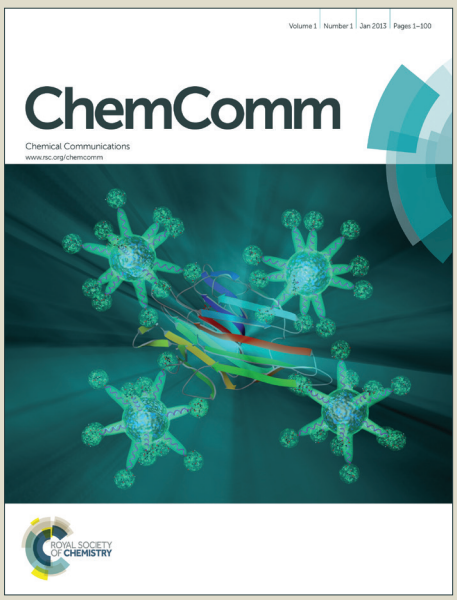

This is an *Accepted Manuscript*, which has been through the Royal Society of Chemistry peer review process and has been accepted for publication.

Accepted Manuscripts are published online shortly after acceptance, before technical editing, formatting and proof reading. Using this free service, authors can make their results available to the community, in citable form, before we publish the edited article. We will replace this *Accepted Manuscript* with the edited and formatted *Advance Article* as soon as it is available.

You can find more information about *Accepted Manuscripts* in the Information for Authors.

Please note that technical editing may introduce minor changes to the text and/or graphics, which may alter content. The journal's standard Terms & Conditions and the Ethical guidelines still apply. In no event shall the Royal Society of Chemistry be held responsible for any errors or omissions in this *Accepted Manuscript* or any consequences arising from the use of any information it contains.

ROYAL SOCIETY OF CHEMISTRY

www.rsc.org/chemcomm

Cite this: DOI: 10.1039/c0xx00000x

www.rsc.org/xxxxxx

ARTICLE TYPE

Controlling and Self Assembling of Monodisperse Platinum Nanocubes as Efficient Methanol Oxidation Electrocatalysts

Xiuhui Sun,[a] Xing Zhu,[b] Nan Zhang,[a] Jun Guo,[b] Shaojun Guo,[c] Xiaoqing Huang[a]*

Received (in XXX, XXX) Xth XXXXXXXXX 20XX, Accepted Xth XXXXXXXXX 20XX

DOI: 10.1039/b000000x

An efficient synthetic approach that enables not only the control of Pt nanocubes but also the one-pot fabrication of novel Pt nanocube assemblies was developed for the first time. The integration of well-defined building blocks and unique superstructures endows Pt nanocube assemblies with enhanced performance in the methanol electrooxidation, showing a new concept for further enhancing the performance of the catalysts.

Platinum (Pt), a key catalyst, plays a significant role in many industrial applications.[1-6] Pt nanostructures serve as the primary catalysts for various chemical conversions and also have remarkable performance in petroleum reforming, gas sensing and fuel cells.[1-6] Although the high performances of Pt nanocatalysts have been demonstrated in various areas, their practical applications seem to have encountered great difficulties in the aspect of the high consumption of scarce Pt in the catalysts.[7-9] Fortunately, theoretical predictions and various experimental studies have suggested that the properties of Pt nanocrystals can be tuned by their particle size and shape.[10-12] In the past decades, extensive research efforts have focused on the size and shape control for Pt nanocrystals.[13-15] The successful synthesis of Pt nanocrystals with desirable size and shape has made readily the Pt nanocrystals with improved utilization of expensive Pt.[16-19]

For the practical applications, however, it has been gradually realized that the performance of nanocrystals depends on not only size/shape but also the arrangement of the nanocrystals.[20-23] The nanostructures with desirable assembling manner usually show enhanced performance as a result of their collective electronic, optical, and magnetic properties being distinctly different from the corresponding individual building blocks.[20-23] After the work by Murray et al. on the assembling of PtFe in 1995,[24] a variety of strategies have been developed by many researchers to assembly a wide range of compositions, such as Pt, Ag, PtFe, CdS, et al.[25-32] Despite the above successful demonstrations, it should be pointed out that previous method for assembling has focused on the "post treatment" strategy. These post treatment strategy, i.e. nanostructure synthesis and the following assembling, however, are neither cost-effective nor efficient.

The simultaneous realization of shape-controlling and assembling of Pt nanostructures thus seems natural and extremely beneficial for the maximization the performance of Pt catalysts. To achieve this, the development of approach for preparing such unique superstructure via an efficient preparation method while exhibiting superior performance is critical. Herein, we report an effective strategy that selectively produces highly monodisperse Pt nanocubes and unique assembled Pt nanocubes in one-pot. The synthetic strategy is based on the combined introduction of formaldehyde and Fe^{3+} into the synthesis, which is most critical to the successful formation of the unique Pt nanocube assemblies. While formaldehyde functions as the surface-confining agent to allow anisotropic growth of the Pt nanocubes as building blocks, the trivalent cation Fe^{3+} is responsible for the formation of unique Pt nanocube assemblies. Furthermore, we have demonstrated that the unique Pt nanocube assemblies exhibit high activity for the methanol electrooxidation with much better performance than those of the monodisperse Pt nanocubes and also the commercial Pt black. Our results indicate that the simultaneous controlling and assembling of the Pt nanocrystals is indeed a very effective strategy to further optimize the performance of the Pt catalysts.

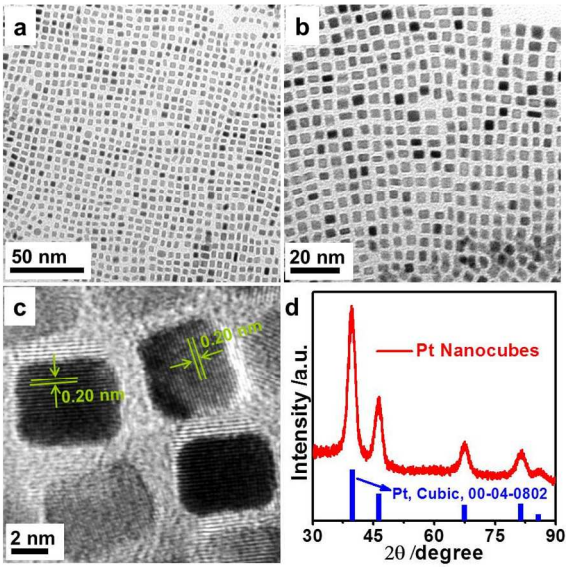

Fig. 1. Morphological and structural analyses for Pt nanocubes. Representative (a) low-magnification TEM, (b) high-magnification TEM and (c) HRTEM images of the Pt nanocubes. (d) PXRD pattern of the Pt nanocubes.

In a typical preparation of the monodisperse Pt nanocubes, platinum acetylacetonate [$Pt(acac)_2$], polyvinylpyrrolidone (PVP), formaldehyde (CH_2O) aqueous solution and benzyl alcohol ($C_6H_5CH_2OH$) were added to a Teflon-lined stainless-

ChemComm Accepted Manuscript

steel autoclave (see Supporting Information for details). After the autoclave had been capped, the mixture was stirred for around 15 minutes to form a homogeneous solution. The sealed vessel was then heated from room temperature to 150 °C and kept at 150 °C for 10 hours in an oven before it was cooled to room temperature. The resulting colloidal products were collected by centrifugation and washed three times with an ethanol (1mL) + acetone (8mL) mixture.

The representative electron microscopic images of the obtained products are presented in **Fig. 1**. The typical transmission electron microscope (TEM) images show that the products consist of uniform nanocrystals with completely cubic morphology, showing the high-yield preparation of the nanocubes (**Fig. 1a**, **Fig. S1**). Those nanocubes are highly monodisperse with an average edge length of 5.3 nm (**Fig. 1b**). The high-resolution TEM (HRTEM) image indicates that the nanocubes are single crystals with well-defined fringes (**Fig. 1c**). The lattice spacing along the edge of the nanocube is 0.20 nm, consistent with the (200) lattice spacing of the face-centered cubic (fcc) Pt, showing that the Pt nanocubes are bounded by the (100) facets. The microstructure of the obtained nanocrystals was also characterized by powder X-ray diffraction (PXRD). The PXRD pattern of the colloidal products displays typical peaks which can be indexed as fcc Pt (JCPDS no. 04-0802), confirming the successful formation of metallic Pt products (**Fig. 1d**).

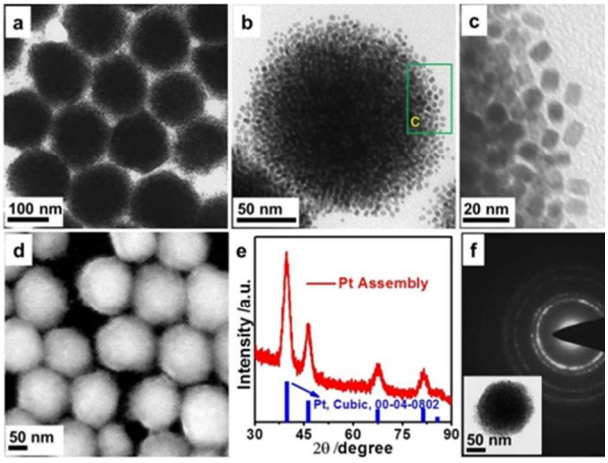

Fig. 2. Representative (a) low-magnification TEM, (b) high-magnification TEM with a box around the portion shown in (c), (c) enlarged high-magnification and (d) HAADF-STEM images of as-prepared Pt nanocube assemblies. (e) PXRD pattern of the Pt nanocube assemblies. (f) SAED pattern of an individual Pt nanocube assembly. Inset in (f) shows the corresponding TEM image.

The use of formaldehyde is of essential importance for the controlling of monodisperse Pt nanocubes. As shown in **Fig. S2a-b**, the reaction in the absence of formaldehyde cannot yield nanocubes. The resultant consists of mainly polyhedra with a diameter of around 8 ± 3 nm. We further found that a critical amount of formaldehyde was found to play an important role in obtaining the monodisperse Pt nanocubes. **Fig. S2c-f** shows TEM images of the reaction products prepared with different amount of formaldehyde. The reactions supplied with neither reduced nor increased amount of formaldehyde lead to nanocubes with reduced quality. Since Pt nanocubes can be produced once the formaldehyde was supplied, we thus consider that formaldehyde is the main contributor for the controlling of Pt nanocubes. In the synthesis, we also found that the use of benzyl alcohol is also critical to the successful synthesis of monodisperse Pt nanocubes. As observed by the TEM images (**Fig. S2g-h**), when we changed benzyl alcohol with DMF, another widely used solvent, in the synthesis and all other experimental conditions were kept the same only small particles mixed with some nanocubes or heavily aggregated nanoparticles were obtained.

The more interesting result is that if additional $FeCl_3$ was introduced into the synthesis of Pt nanocubes while all the other details were kept the same, the reaction leads to the formation of unique Pt nanocube assemblies (**Fig. 2**, **Fig. S3**). The product consists of uniform nanostructures with a nearly spherical outline at the first glance, as confirmed by the typical low-magnification TEM image (**Fig. 2a**). Those spherical nanostructures are highly uniform with diameters ranging from 138 nm to 176 nm (average of 152 nm). Remarkably, each spherical nanostructure surveyed is a supercrystal with many small subunits. The small subunits are small nanocubes, as revealed by the enlarged high-magnification TEM image (**Fig. 2b-c**). The superstructural feature of the nanostructures is clearly presented by the high-angle annular dark-field scanning TEM (HAADF-STEM) image (**Fig. 2d**, **Fig. S3**). The microstructure of the obtained products was further analyzed by PXRD. The PXRD pattern of the products (**Fig. 2e**) shows one distinct set of diffraction peaks assigned to the fcc structures of Pt, confirming the formation of metallic Pt in the products. No detectable impurity peaks are observed from the PXRD pattern, confirming that only a single Pt phase exists in the products. The crystalline nature of the obtained Pt nanocube assemblies was also analyzed by selected area electron diffraction (SAED) and HRTEM image (**Fig. 2f**, **Fig. S4**). The SAED pattern on a single Pt nanocube assembly shows concentric rings composed of bright discrete diffraction spots that can be indexed to crystal planes of fcc Pt. The HRTEM image, as shown in **Fig. S4**, reveals that the building blocks of the assemblies are Pt nanocubes. Thus, all the data support the formation of unique Pt nanocube assemblies. Together, we have developed a simple and efficient approach to selectively produce monodisperse Pt nanocubes and unique Pt nanocube assemblies.

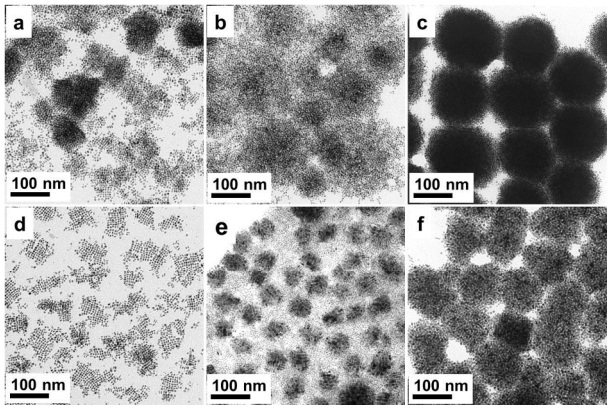

Fig. 3. Typical TEM images of Pt nanostructures prepared using the standard procedure for the preparation of Pt nanocube assemblies, except for the use of different amount of $FeCl_3$: (a) 1.35 mg, (b) 2.7 mg and (c) 13.5 mg. TEM images of Pt

ChemComm Accepted Manuscript

This journal is © The Royal Society of Chemistry [year]

nanostructures prepared using the standard procedure for the preparation of Pt nanocube assemblies, except for changing $FeCl_3$ with (d) NaCl, (e) $MnCl_2$ and (f) $CoCl_3$.

Since $FeCl_3$ appears to be the most critical reagent for the formation of Pt nanocube assemblies, we have studied its role in details. Without the introduction of $FeCl_3$, monodisperse Pt nanocubes with no assembling behaviour were obtained, as demonstrated in **Fig. 1**. When the amount of $FeCl_3$ was increased to 1.35 mg, Pt nanocubes began to assemble into aggregates to some extent (**Fig. 3a**, **Fig. S5**). The assembling feature of the Pt nanocubes became obvious as the amount of $FeCl_3$ was increased to 2.7 mg (**Fig. 3b**). When the concentration of $FeCl_3$ was further increased to 6.75 mg, unique Pt nanocube assemblies were produced (**Fig. 2**). The structure was almost unaffected by increasing the amount of $FeCl_3$ from 6.75 to 13.5 mg (**Fig. 3c**). When $FeCl_3$ was replaced by the same amount of $Fe(NO_3)_3$, Pt nanocube assemblies similar to the typical products were formed (**Fig. S6**). It can be therefore concludes that Fe^{3+} cations control the assembling behaviour of the Pt nanocubes, and increasing the amount of Fe^{3+} cation facilitates their assembly to unique Pt nanocube assemblies.

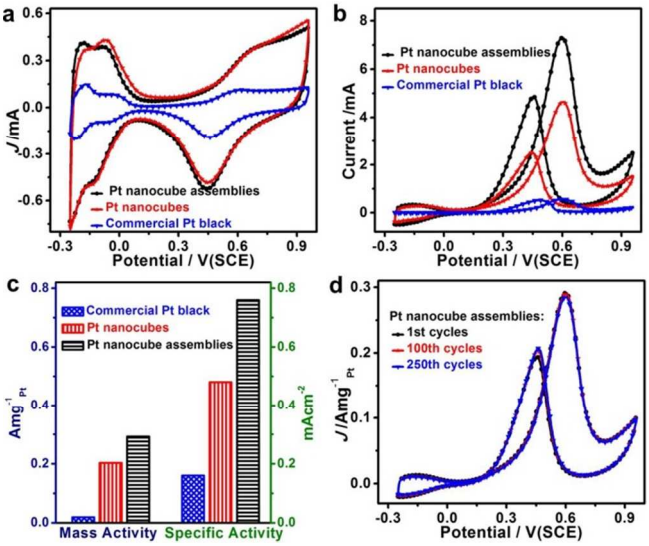

Fig. 4. Electrocatalytic properties of the Pt nanocube assemblies, Pt nanocubes and commercial Pt black. (a) Cyclic voltammograms recorded at room temperature in 0.1 M $HClO_4$ aqueous solution (50 mV s^{-1}). (b) Methanol oxidation curves recorded at room temperature in a 0.1 M $HClO_4$ + 0.2 M methanol aqueous solution (50 mV s^{-1}). (c) Specific activity and mass activity of these three catalysts, which are given as current densities normalized to the EASA and the loading amount of Pt, respectively. (d) Cyclic voltammograms (1st, 100th and 250th cycle) of Pt nanocube assemblies for methanol oxidation. Potential was continuously scanned between 0.05 and 1.26 V *vs* reversible hydrogen electrode (RHE) for 250 cycles at 50 mV s^{-1} in 0.1 M $HClO_4$ + 0.2 M methanol.

In many previous studies, the use of charged additives, especially cations, has been demonstrated to be an effective strategy to control the assembly of nanocrystals.[33-36] Previous work has demonstrated that the assembly of biomolecules follows the theory of counterion condensation. The folding efficiency of RNA by using divalent cations is stronger than those of monovalent cations.[37-38] To gain insight into the role of Fe^{3+} in the control of Pt nanocube assemblies, additional control experiments by changing $FeCl_3$ with other commonly used chlorides while keeping the other parameters the same were carried out. As shown in **Fig. 3d-f** and **Fig. S5**, NaCl was not able to assemble the monodisperse Pt nanocubes. In contrast, when $FeCl_3$ was replaced by the same amount of $CoCl_3$, Pt nanocube assemblies were formed. Pt assemblies mixed with isolated Pt nanocubes were obtained when $FeCl_3$ was substituted by $MnCl_2$. The assembling ability of the cations in our system are in the order of trivalent Fe^{3+}, Co^{3+}>bivalent Mn^{2+}>monovalent Na^+. The trivalent cations show the largest assembling ability, which is consistent with previous results.[35] Thus, the introduction of high concentration and trivalent cations are responsible for the *in-situ* formation of unique Pt nanocube assemblies by this method.

The obtained unique Pt nanostructures were studied by their electrochemical properties by using the methanol electrooxidation as a probe reaction. Before the measurements, a simple ethanol + acetone wash (4 times) was applied to remove the bulky capping agents on the surface of the nanostructures. The treated nanostructures were redispersed in ethanol for the electrochemical tests. Small portion of this dispersion was deposited on the surface of glassy carbon electrode and dried under ambient conditions.

Electrochemical measurements were carried out using the standard three-electrode setup with a saturated calomel electrode (SCE) and Pt wire as the reference and counter electrodes, respectively (see the Experimental Section). Cyclic voltammetry (CV) was used to evaluate the electrochemically active surface area (EASA) of the Pt catalysts. A commercial Pt black catalyst was used as reference (Aldrich, 205915-1G, **Fig. S7**). **Fig. 4a** compares the CV curves on these three different catalysts recorded in 0.1 M $HClO_4$ aqueous solution at a sweep rate of 50 mVs^{-1}. The Pt mass loadings of Pt nanocube assemblies, Pt nanocubes and commercial Pt black catalysts were 25.5 μg, 23.2 μg and 30.0 μg, respectively. The EASA was calculated by measuring the charge collected in the hydrogen adsorption/desorption region after double-layer correction and assuming a value of 210 μCcm^{-2} for the adsorption of a hydrogen monolayer. The Pt nanocube assemblies and monodisperse Pt nanocubes display EASA of 40.5 m^2g^{-1} and 42.3 m^2g^{-1}, respectively, which is much higher than that of commercial Pt black (10.8 m^2g^{-1}).

The methanol electrooxidation measurements were carried out in the electrolytes of 0.1 M $HClO_4$ + 0.2 M CH_3OH at room temperature. **Fig. 4b** shows the electrooxidation curves for three different catalysts. In order to compare the activity, the currents were further normalized with respect to both the electrochemically active surface area and the mass loading of Pt. As shown in **Fig. 4c**, the Pt nanocube assemblies catalyst exhibited a mass activity of 0.292 A/mg_{Pt} at 0.6 V, which was 1.44 and 15.1 times greater than that of the monodisperse Pt nanocubes (0.203 A/mg_{Pt}) and the commercial Pt black catalyst (0.0185 A/mg_{Pt}), respectively. The specific activities of the above different catalysts also showed similar behaviour to that of the mass activities. The Pt nanocube assemblies (0.76 $mAcm^{-2}$) had a specific activity of 1.58 and 4.21 times that of the monodisperse

ChemComm Accepted Manuscript

Pt nanocubes catalyst (0.48 $mAcm^{-2}$) and commercial Pt black catalyst (0.18 $mAcm^{-2}$), respectively. In addition, the durability of the Pt nanocube assemblies, Pt nanocubes and commercial Pt black were tested by repeating the CV sweeps for 250 cycles (**Fig. 4d** and **Fig. S8**). The activities of both Pt nanocube assemblies and Pt nanocubes remained much higher than commercial Pt black even after 250 sweeping cycles. After 250 sweeping cycles, 96.5% of the initial catalytic activity was still maintained for Pt nanocube assemblies, as compared with the loss of 9.9 % for Pt nanocubes and 22.8% for commercial Pt black, respectively, highlighting a much better catalytic performance of the unique Pt nanocube assemblies. The enhanced properties of Pt nanocube assemblies reported herein are likely due to the combination of the shape effects and synergistic effects between the building blocks.[22]

Conclusions

We have developed a facile strategy for the preparation of Pt nanocubes with a controllable assembling manner. Monodisperse Pt nanocubes and Pt nanocube assemblies have been selectively obtained in high yield. The combined use of formaldehyde and Fe^{3+} is critical to the successful formation of the Pt nanocube supercrystals in one pot. While formaldehyde functions as the surface-confining agent to control the growth of the uniform Pt nanocubes as the building blocks, the trivalent cation Fe^{3+} is responsible for the formation of unique Pt nanocube assemblies. All the synthesis reagents were fully optimized for the synthesis of monodisperse Pt nanocubes and Pt nanocube assemblies. We further showed that the unique Pt nanocube assemblies served as highly efficient catalysts in the electrooxidation of ethanol with better performance than those of the monodisperse Pt nanocubes and commercial Pt black. The enhanced catalytic properties could be attributed to the combination of shape effects and synergistic effects between the building blacks. The present study indicates that the simultaneous controlling and assembling of the Pt nanocrystals is indeed a potential strategy to further optimize the properties of the Pt catalysts.

This work was financially supported by the start-up funding from Soochow University, Young Thousand Talented Program and J. Robert Oppenheimer Distinguished Fellowship.

Notes and references

[a] *College of Chemistry, Chemical Engineering and Materials Science, Soochow University, Jiangsu 215123, China.*
E-mail: hxq006@suda.edu.cn
[b] *Testing & Analysis Center, Soochow University, Jiangsu, 215123, China*
[c] *Physical Chemistry and Applied Spectroscopy, Los Alamos National Laboratory, Los Alamos, New Mexico, 87545, U. S. A.*

† Electronic Supplementary Information (ESI) available: [details of any supplementary information available should be included here]. See DOI: 10.1039/b000000x/

1 J. Tollefson, *Nature* 2008, **451**, 877.
2 M. K. Debe, *Nature* 2012, **486**, 43.
3 B. Lim, M. J. Jiang, P. H. C. Camargo, E. C. Cho, J. Tao, X. M. Lu, Y. M. Zhu, Y. N. Xia, *Science* 2009, **324**, 1302.
4 Y. Yamada, C. K. Tsung, W. Huang, Z. Y. Huo, S. E. Habas, T. Soejima, C. E. Aliaga, G. A. Somorjai, P. D. Yang, *Nat. Chem.* 2011, **3**, 372.
5 A. C. Chen, P. Holt-Hindle, *Chem. Rev.* 2010, **110**, 3767.
6 S. J. Guo, S. Zhang, S. H. Sun, *Angew. Chem., Int. Ed.* 2013, **52**, 8526.
7 H. A. Gasteiger, N. M. Markovic, *Science* 2009, **324**, 48.
8 F. A. De Bruijn, V. A. T. Dam, G. J. M. Janssen, *Fuel Cells* 2008, **8**, 3.
9 H. A. Gasteiger, S. S. Kocha, B. Sompalli, F. T. Wagner, *Appl. Catal., B* 2005, **56**, 9.
10 N. Tian, Z. Y. Zhou, S. G. Sun, *J. Phy. Chem. C* 2008, **112**, 19801.
11 Z. L. Wang, *J. Phy. Chem. B* 2000, **104**, 1153.
12 J. Oliver-Meseguer, J. R. Cabrero-Antonino, I. Dominguez, A. Leyva-Perez, A. Corma, *Science* 2012, **338**, 1452.
13 H. Zhang, M. Jin, Y. Xia, *Chem. Soc. Rev.* 2012, **41**, 8035.
14 N. S. Porter, H. Wu, Z. Quan, J. Fang, *Acc. Chem. Res.* 2013, **46**, 1867.
15 J. Wu, H. Yang, *Acc. Chem. Res.* 2013, **46**, 1848.
16 N. Tian, Z. Y. Zhou, S. G. Sun, Y. Ding, Z. L. Wang, *Science*, 2007, **316**, 732.
17 S. E. Habas, H. Lee, V. Radmilovic, G. A. Somorjai, P. D. Yang, *Nat. Mater.* 2007, **6**, 692.
18 B. Lim, M. J. Jiang, P. H. C. Camargo, E. C. Cho, J. Tao, X. M. Lu, Y. M. Zhu, Y. N. Xia, *Science* 2009, **324**, 1302.
19 W. Si, J. Li, H. Li, S. Li, J. Yin, H. Xu, X. Guo, T. Zhang, Y. Song, *Nano Research* **2013**, 6, 720.
20 M. R. Jones, K. D. Osberg, R. J. Macfarlane, M. R. Langille, C. A. Mirkin, *Chem. Rev.* 2011, **11**, 3736.
21 Y. Bae, N. H. Kim, M. Kim, K. Y. Lee, S. W. Han, *J. Am. Chem. Soc.* 2008, **130**, 5432.
22 J. Henzie, M. Grünwald, A. Widmer-Cooper, P. L. Geissler, P. Yang, *Nat. Mater.* 2012, **11**, 131.
23 Y. Kang, X. Ye, J. Chen, Y. Cai, R. E. Diaz, R. R. Adzic, E. A. Stach, C. B. Murray, *J. Am. Chem. Soc.* 2013, **135**, 42.
24 C. B. Murray, C. R. Kagan, M. G. Bawendi, Science 1995, 270, 1335.
25 S. H. Sun, C. B. Murray, D. Weller, L. Folks, A. Moser, *Science* 2000, **287**, 1989.
26 F. X. Redl, K. S. Cho, C. B. Murray, S. O'Brien, *Nature* 2003, **423**, 968.
27 F. Dumestre, B. Chaudret, C. Amiens, P. Renaud, P. Fejes, *Science* 2004, **303**, 821.
28 D. V. Talapin, C. B. Murray, *Science* 2005, **310**, 86.
29 E. V. Shevchenko, D. V. Talapin, N. A. Kotov, S. O'Brien, C. B. Murray, *Nature* 2006, **439**, 55.
30 D. K. Smith, B. Goodfellow, D. M. Smilgies, B. A. Korgel, *J. Am. Chem. Soc.* 2009, **131**, 3281.
31 A. G. Dong, J. Chen, P. M. Vora, J. M. Kikkawa, C. B. Murray, *Nature* 2010, **466**, 474.
32 K. Miszta, J. de Graaf, G. Bertoni, D. Dorfs, R. Brescia, S. Marras, L. Ceseracciu, R. Cingolani, R. van Roij, M. Dijkstra, L. Manna, *Nat. Mater.* 2011, **10**, 872.
33 H. Zhang, D. Y. Wang, *Angew. Chem., Int. Ed.* 2008, **47**, 3984.
34 W. Y. Li, P. H. C. Camargo, L. Au, Q. Zhang, M. Rycenga, Y. N. Xia, *Angew. Chem., Int. Ed.* 2010, **49**, 164.
35 Y. Z. Liu, X. M. Lin, Y. G. Sun, T. Rajh, *J. Am. Chem. Soc.* 2013, **135**, 3764.
36 C. Hu, K. Lin, X. Wang, S. Liu, J. Yi, Y. Tian, B. Wu, G. Chen, H. Yang, Y. Dai, H. Li, N. Zheng, *J. Am. Chem. Soc.* 2014, **136**, 12856.
37 S. L. Heilman-Miller, D. Thirumalai, S. A. Woodson, *J. Mol. Biol.* 2001, **306**, 1157.
38 G. C. L. Wong, L. Pollack, *Annu. Rev. Phys. Chem.* 2010, **61**, 171.

ChemComm Accepted Manuscript

This journal is © The Royal Society of Chemistry [year]